

Comparative Study of Optical and Radio-Frequency Communication Systems for a Deep-Space Mission

H. Hemmati, K. Wilson, M. K. Sue, L. J. Harcke, M. Wilhelm, C.-C. Chen, J. Lesh, and Y. FERIA
Communications Systems and Research Section

D. Rascoe and F. Lansing
Spacecraft Telecommunications Equipment Section

J. W. Layland
Telecommunications Science and Engineering Division

We have performed a study on telecommunication systems for a hypothetical mission to Mars. The objective of the study was to evaluate and compare the benefits that microwave—X-band (8.4 GHz) and Ka-band (32 GHz)—and optical communications technologies afford to future missions. The telecommunication systems were required to return data after launch and in orbit at 2.7 AU with daily data volumes of 0.1, 1.0, or 10.0 Gbits (Gb). Spacecraft terminals capable of delivering each of the three data volumes were proposed and characterized in terms of mass, power consumption, size, and cost. The estimated parameters for X-band, Ka-band, and optical frequencies are compared and presented here. For all cases, the optical flight terminal exhibits about 60 percent of the mass of the corresponding radio frequency (RF) subsystem. Power consumption is comparable for all three technologies at a 0.1 Gb/day data volume, but the power required at either Ka-band or optical is less than half of the X-band requirement at 10 Gb/day. These benefits can be obtained only with a suitable investment in reception facilities for Ka-band or optical frequencies.

As part of an overall study plan to examine the future of space communications across the solar system, we explored the application of these three design points for other possible destinations and, in particular, for Neptune. Although the data return capability at Neptune is reduced by over two orders of magnitude from the Mars case, the relative comparison between the three bands is little changed.

I. Introduction

The Advanced Communications Benefits Study (ACBS) was started in late 1994 to examine the benefits that would accrue from successful pursuit of the ongoing technology development for Ka-band (32 GHz) and optical communications elements. The baseline for comparison is the current X-band (8.4-GHz) system, as used for Voyager, Mars Observer (MO), and Mars Global Surveyor (MGS). The

first leg of this study, to be described in the following, considered a hypothetical series of missions to Mars, missions for which the communications elements could be identical even though the science data would change. Early results of this leg of the study have been presented at the Society of Photo-Optical Instrumentation Engineers (SPIE) conference in February 1996 [7]. These will be summarized in the following, along with the more recent products of the study.

Historically, the migration toward higher frequencies by the Deep Space Network (DSN) and the spacecraft it supports has been the most significant single factor in the steady growth of deep-space communications capability. L-band (900 MHz) and S-band (deep-space allocation 2.29- to 2.30-GHz) frequencies were used throughout the 1960's. In 1977, X-band (8.4 GHz) was put to use as the prime downlink for the twin Voyager spacecraft after experimental packages flown on the Mariner Venus-Mercury and Viking missions of the early 1970's demonstrated the viability of the frequency. In the 1990's, NASA has committed to the idea of flying smaller spacecraft with targeted science payloads. Extending the space-Earth communication frequency to Ka-band (32 GHz) will allow NASA to save spacecraft mass and power while achieving the same data return volumes that X-band provides. Ka-band experimental packages on the Mars Observer, Cassini, and Mars Global Surveyor spacecraft are helping to establish the viability of Ka-band for future deep-space communication uses. Use of optical frequencies is expected to afford further savings on mass and power consumption.

Comparisons have been made at three distinct performance levels for the (hypothetical) Mars missions, each having the capability for an expected (probabilistic) daily data return of 0.1, 1.0, or 10.0 Gbits (Gb) per day into a single ground terminal. For each of the three performance levels and each of the frequency bands, feasible flight designs and ground configurations are developed and used for comparison of characteristics, such as power, mass, and development and operating costs.

The choice of this span of performance levels, rather than using a specific mission model, was made in the hopes of establishing some fairly general conclusions that would be robust in spite of changes to actual plans for future missions. The 0.1 or 1.0 Gb/day is in the neighborhood of current mission planning. The 10.0 Gb/day was chosen at the start of the study as a stretching "what-if" that went beyond any of the then-current small mission plans. Recent "roadmap" studies for a revitalized space exploration program make this appear far too conservative.

The assumed mission scenario consists of a 6-month interval at Mars, starting at the minimum Sun-Earth-probe (SEP) angle permitted by the technology. Device lifetime is specified as 5 years in order to offer high confidence that all would be operating at least through the cruise to Mars plus the 6-month prime mission. If our experience is a guide, spacecraft survival beyond its prime mission will lead to an extended mission with lessened data flow, but this is neither guaranteed nor included in the cost planning for the prime mission. The spacecraft is assumed to have an onboard intelligence capable of recovering from any tumbling event and acquiring Earth-point to within a specified 0.1-deg attitude. Thus, no traditional low-gain antenna or emergency command function is included. Also assumed is a large onboard storage capacity able to hold on the order of a week of data and to ensure that no gathered data are lost through interruption of the downlink data flow. Both assumptions are pivotal in making optical communications a viable option. Adding a requirement for low-rate emergency communications nearly independent of spacecraft attitude would appear to force the inclusion of a small radio-frequency (RF) element in all configurations. Also, eliminating the use of onboard storage for covering weather-induced outages in communications would significantly increase the needed investment in Earth-based optical telecommunications terminals.

To help constrain the extent of technological futurology involved in the study, the technology "freeze" date was set at December 1996 for a technology readiness level of at least 4 (component or breadboard validation in a laboratory environment). Note that the RF components are in fact at a much higher level, representing flight engineering models or actual flight hardware, so some improvements in mass, power, and efficiency should be attainable. Costing is based on fixed-value 1995 dollars. No actual cost figures

are included in the current article, but relative (normalized) cost values are used in comparison of the various telecommunications systems.

One of the initial motivations for this study was to be able to recommend the appropriate domain(s), based on mission characteristics, for use of each of the candidate frequency bands. Destinations of interest include not just Mars but span distances from the Earth–Luna neighborhood to the far outer planets like Neptune and Pluto. While the bulk of the work described here applies strictly to Mars, there is included an initial look at other destinations, and Neptune in particular, using as a basis the designs devised for the Mars missions. Although the data return capability at Neptune is reduced by over two orders of magnitude from the Mars case, the relative comparison between the three frequency bands is little changed. In essence, the relative merits of the bands have much to do with the investment in telecommunications infrastructure and with the dynamics of weather effects upon the link, in addition to the basic dependence upon direct link performance.

A. General Considerations

There are four main considerations that tend to apply in different specific ways to these frequency bands. These are

- (1) The technological maturity of the equipment for handling the signals.
- (2) The choice of an operations concept appropriate to the mission needs and the signal propagation effects.
- (3) The infrastructure investment in the ground terminals for handling the signals.
- (4) The flight terminal parameters: mass, power, and cost.

All four of these can be translated into economic terms, although some are more directly handled than others. Each will be addressed in turn for each of the three frequency bands.

1. Technological Maturity. The X-band capability is currently well established, having been the operational frequency of the Voyager spacecraft and the frequency of choice for most following spacecraft. It is a mature technology, and technology investment continues to improve efficiency and cost factors. The Ka-band capability is currently reaching a “level 7” as an experimental transmitting capability and will soon be demonstrated with a flight on MGS, and a gravitational wave radio science experiment will fly on Cassini in 1997. Technology investment also continues to improve its efficiency and cost factors. Optical communications for deep space is well on its way as an experimental technology but still requires substantial investment before it could become the primary communications channel for a mission. Demonstrations such as the Galileo Optical Experiment (GOPEX) [3] and the Ground/Orbiter Lasercomm Demonstration (GOLD) [5] have shown hints of the promised capability but also some of the difficulties to be faced in achieving the precision pointing required. Additionally, flight systems have or are being built in the U.S. [10,11], Japan [12,13], and Europe [14]. Further, there are several commercial satellite communications systems’ manufacturers that are planning to use this technology in commercial communications network applications. These developments should add to the maturity index for the technology, but additional tailoring of its parameters and validation of its system-level performance, both in the laboratory and in a deep-space environment, will be required.

2. Operations Concept. Missions supported by the DSN have been accustomed to a worldwide coverage that can be scheduled at any time and is subject to a weather hazard outage of at most a few percent of scheduled coverage. Spacecraft activities can be scheduled based on a mission’s flight trajectory with little concern for time on Earth. DSN station schedules and the schedules of people supporting the mission are chosen to fit the demands of the trajectory. An alternative operations concept arises when all data are stored (temporarily) on the spacecraft and transferred to Earth in a controlled interactive fashion. Data are delivered whenever contact time is scheduled and there is no hazard intervening. Data

that are transmitted but fail to be received correctly are repeated, following some preset protocol, until they have been received successfully. Here the key factor is the net average data volume delivered, without concern for timeliness.

Following the conventional real-time operations concept, a small weather-related margin of a few tenths of a dB is required at X-band to provide acceptable performance with the current DSN. Outages are confined to intervals of active rain. A similar situation applies at Ka-band although the weather-related margin is higher and currently funded plans do not (yet) include implementing Ka-band at all stations. Implementation of two additional Ka-band-capable sites is necessary to achieve full worldwide coverage for real-time operations. Data-volume-driven operations can be achieved via the current single Ka-band site. As desired, the weather margin could be relaxed to optimize the data transport process.

For optical communications, there is a weather hazard on the order of 30 percent from cloud coverage at any single site. The exact value for this hazard level varies with specifics of season and location. Providing for the conventional real-time operations is believed to require concurrent visibility to the spacecraft from three dispersed sites in order to achieve an acceptable hazard level. A single site, presumably in a dry area of the U.S., would be selected for data-volume-driven operations.

3. Infrastructure Investment. The investment required in supporting infrastructure is intimately tied with the selection of an operations concept for each of the three bands. Facilities dispersed fairly uniformly and worldwide are required to achieve the conventional worldwide real-time operations, which is provided at X-band by the current DSN. A modest investment in new facilities would be required for the data-volume-driven operations at any other frequency.

As noted above, the current DSN provides for worldwide real-time X-band coverage. The network can also provide a data-volume-driven style of operations. The DSN currently is implementing Ka-band at a single site for Cassini, and could soon provide a data-volume-driven style of operations. Two additional overseas sites would be required to achieve the conventional operations style.

No operational support facilities currently exist for optical communications. Implementation of a single ground terminal at a suitable site in the Southwestern U.S. would provide for a data-volume-driven style of operations. A study published in 1994 concluded that a network of seven optical ground terminals, suitably dispersed about the world, would be capable of providing for the conventional worldwide real-time operations.¹ Design details of the optical ground terminal appear later in Section III of this article. The design is derived from that used in the above-cited GBAT study.

Ground support equipment (GSE) costs were taken as a nonrecurring cost and included in the cost estimates for the first terminal unit for all three technologies considered. No recurring cost for GSE was included as it was assumed that the GSE developed for the first unit could be used to support subsequent units.

4. Flight Terminal Characteristics. Generally, the steps from X-band to Ka-band to optical provide for reduction in flight terminal mass and power consumption. This is enabled by the enhanced directivity of radiation from an antenna/telescope as the operating wavelength decreases. Tighter tolerances and lower device efficiencies counter this somewhat. In the following sections, specific flight terminal designs are developed, and their mass, power, and cost are estimated for each of the selected capacity levels.

¹ *Ground Based Advanced Technology Study (GBATS)*, JPL D-11000, Release 1 (internal document), Jet Propulsion Laboratory, Pasadena, California, August 5, 1994.

B. Challenges Facing the Study

One of the more difficult challenges facing this study (and others such as this) has been to assure that comparisons are made between systems of equivalent capability and behavior. All systems are assumed to be able to provide telemetry, command, and metric (for navigation) functions. Metric functions at Ka-band will utilize precision Doppler and range and will function the same as at X-band, whereas those at optical frequencies will depend upon precision range and differenced range (and topocentric angles). For RF radio metrics, the switch to Ka-band will increase the intrinsic precision of the measurements and decrease the influence of certain error sources, such as ionosphere and interplanetary media. With no coherent carrier signal available at optical frequencies, the precision metric function would need to be provided through timing information imposed on the data stream and sharing time, power, or bandwidth with the data signal itself. The full impact of this distinction has not been explored and is a recommended topic for future study.

Yet another obstacle has been consideration of operations costs for missions supported at these bands. Distinctions due to the frequency band difference are likely to be obscured by other factors, such as age and level of automation in the ground equipment. Consideration of Ka-band seems fairly direct since the needed equipment is a small increment to the already large investment in the DSN. Forces exist that will lower the operating cost of the network in the future, and one could expect these to affect X-band and Ka-band alike. Optical facilities would be new and presumably would be designed for automatic and unattended operation. Direct estimates for the maintenance and sustaining costs of such an optical facility can and have been made and will be used in a follow-on article² as part of the construct for comparison of overall costs.

Comparison of the estimated costs for similar nonidentical items can be readily obscured by hidden differences in the assumed style of development. Many variations exist along the path from traditional to faster/cheaper without precise words to define the details of the chosen development mode. Accordingly, a cost-model approach was considered in a search for unencumbered cost comparisons for the three communications bands. This cost-model work was done after the designs and the ACBS team's parameter and cost estimates had been completed. Two models were examined. One was the Instrument Cost Model (ICM) used by the Advanced Projects Design Team (Team-X) in the JPL Project Design Center for preliminary cost values for any generic instrument. The model is based predominantly on subsystem mass, with no specific provision for heritage, technical maturity, or complexity. The designers' estimates generally were lower than the nominal cost-model values but were statistically consistent with being members of the ensemble of instruments that forms the basis of the model. The other model was developed and utilized by the JPL Resource and Strategic Planning Group and derived from JPL's accumulated experience with flight projects and instruments over the past 30 years.³ Applied only to the 10-Gb/day first flight units, the resultant cost-model estimates generally fell within an anticipated (allowable) 20 percent of the designers' cost estimates, signaling an apparent confirmation.

We will present the descriptions and comparisons of the RF links performance and relative costs at X- and Ka-band in Section II and of the optical link in Section III. Section IV contains a brief summary of application of the Mars design point to other destinations, such as Neptune. An overall summary will be given in Section V.

² C. Chen, Y. Feria, L. Harcke, H. Hemmati, F. Lansing, J. Layland, L. Lesh, D. Rascoe, M. Sue, M. Wilhelm, and K. Wilson, "Comparative Study of Optical and Radio Frequency Communication Systems for a Mars Mission—Part II," in preparation.

³ G. Ball, R. Levin, and J. Oliverie, "Advanced Communication Benefit Study—Optical Transceiver Cost Estimates," JPL Interoffice Memorandum 311.1-95-017 (internal document), Jet Propulsion Laboratory, Pasadena, California, April 21, 1995.

II. X-Band and Ka-Band Communication

A. RF Design Methodology

A spacecraft radio communication system supports command, telemetry, and radio metric tracking (navigation) functions. Since the downlink data rate requirement for the return of science and navigation digital imaging is much greater than the uplink requirement for commands to the flight computer, the downlink data rate drives the system design. The design approach followed in this study was to minimize the total impact of the telecommunications subsystem by minimizing the cost of the radio system first, and then its mass and power consumption. The rigid parabolic reflector antenna and transponders comprise most of the system mass, while the RF transmitter consumes the majority of power. A database containing several sizes of antennas and power amplifiers was established. These candidate subsystems were taken from a combination of heritage designs and concept designs for other missions, including Cassini, Mars Global Surveyor, Mars Pathfinder, Pluto Express, and the Space Infrared Telescope Facility. Subsystems were selected from the database to create a design that would satisfy the link requirements. X-band (7.2 GHz) was used for the uplink in all designs. Two different downlink frequencies, X-band (8.4 GHz) and Ka-band (32 GHz), were examined as shown in Table 1.

To meet the daily volume requirements of 0.1, 1.0, or 10.0 Gb/day, the RF link design assumed one track a day using one NASA DSN 34-m antenna. A worst-case Earth–Mars range of 2.7 astronomical units (AU) was used, as would be seen during the Mars superior conjunction of August 2002. The downlink channel uses a (15,1/6) inner convolutional code concatenated with a Reed–Solomon (255,223) outer code with an interleaving depth five requiring a 0.9-dB bit signal-to-noise ratio (SNR) at the output of the Reed–Solomon (RS) decoder for a bit-error rate (BER) of 10^{-5} . This is equivalent to a 0.3-dB bit SNR at the output of the Viterbi decoder, which is observed by DSN station operators.

Table 1. RF downlink budgets for a 1.0-Gb/day data volume.

Item	X-band		Ka-band	
	Design	Variance	Design	Variance
RF power, dBm (W)	39.0 (8.0)	0.04	33.2 (2.1)	0.04
Circuit loss, dB	−0.5	0.01	−0.3	0.01
Spacecraft antenna gain, dBi	39.6 (1.4 m)	0.04	50.8 (1.4 m)	0.04
Spacecraft pointing loss, dB	−0.04	0.00	−0.5	0.11
Space loss (2.7 AU), dB	−283.1	0.00	−294.7	0.00
Atmospheric attenuation, dB	−0.11	0.00	−0.4	0.01
Ground pointing loss, dB	−0.10	0.00	−0.3	0.03
G/T, dB/K	53.9	0.01	61.9	0.01
Boltzman’s constant, dB-mJ/K	−198.6	—	−198.6	—
Total power-to-noise ratio, dB-Hz	47.3	0.12	48.3	0.36
Data rate, dB-Hz (kbps)	45.5 (35.8)	—	46.3 (43.2)	—
System loss, dB	−0.4	0.01	−0.4	0.01
Bit signal-to-noise E_b/N_0 , dB	1.8	0.12	1.9	0.36
Required E_b/N_0 (BER = 10^{-5}), dB	0.3	—	0.3	—
Link margin, dB	1.1	0.12	1.3	0.36

B. Ground Antenna Description

The ground antenna systems used for the mission-set comparison are the 34-m-diameter X-band high-efficiency (HEF) antenna and the new 34-m-diameter beam-waveguide (BWG) antenna currently under construction for the DSN. The BWG antenna, shown in Fig. 1, is capable of simultaneous X-/Ka-band uplink/downlink operation through the use of a dichroic plate diplexer. The microwave receiver packages at both antennas consist of cooled high electron mobility transistors (HEMTs). The expected gain/temperature (G/T) performance values for these antennas are 53.9 dB/K for a 34-m HEF antenna at X-band and 61.9 dB/K for a 34-m BWG antenna at Ka-band, assuming a 30-deg elevation angle and 90-percent weather availability. The X-band uplink and downlink capabilities currently exist on these antennas. Implementation of a Ka-band downlink is now under way at one Goldstone antenna to support a Cassini radio science experiment.

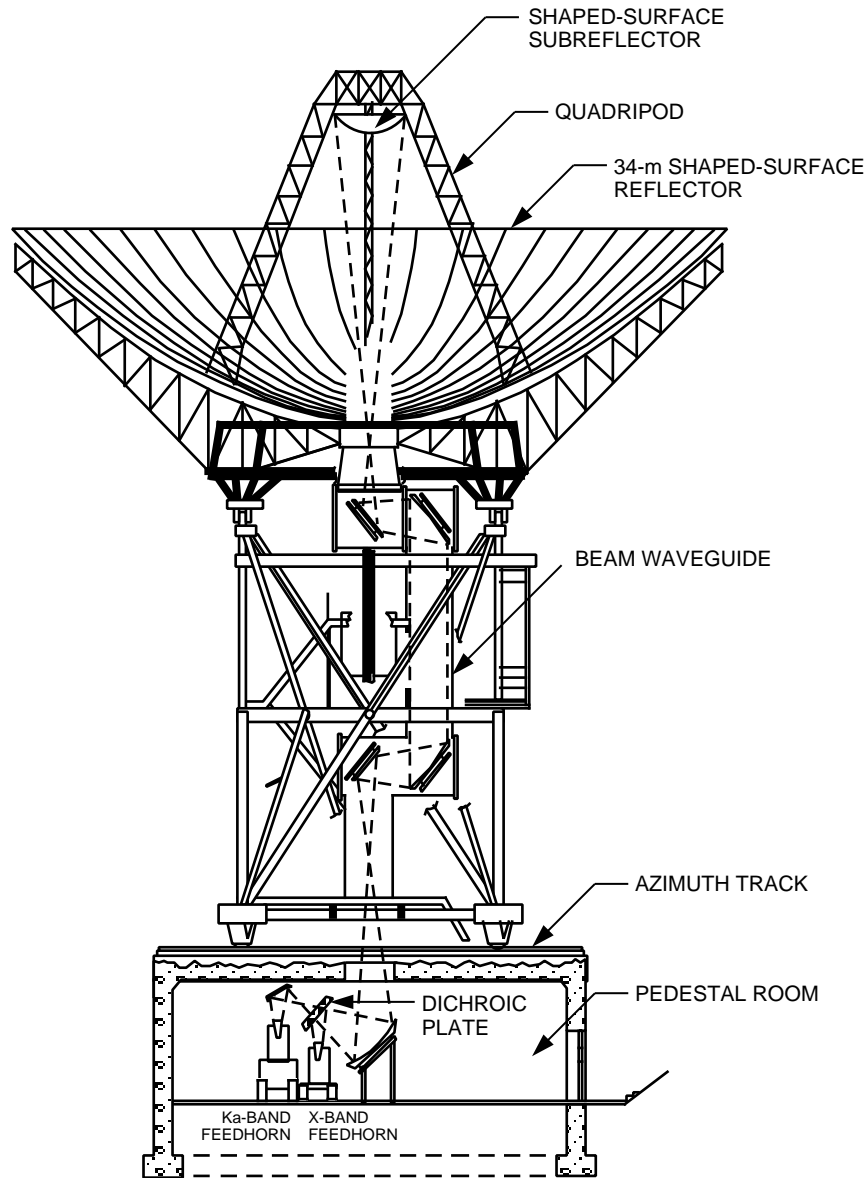


Fig. 1. Schematic of the 34-m beam-waveguide antenna.

C. RF Telecommunications Hardware Systems

The spacecraft RF telecommunications system is usually comprised of three major subsystems: antenna, high power amplifier (HPA), and transponder. Each of these subsystems has several major components. For example, the antenna subsystem has at least a high-gain antenna (HGA) and a low-gain antenna (LGA) for emergency or uplink purposes. The transponder subsystem consists of a receiver and an exciter, and the high-power amplifier can be a traveling-wave tube power amplifier (TWTA) or a solid-state power amplifier (SSPA). For the purpose of this study, two RF telecommunications systems options were evaluated: the first was an X-band up/X-band down (X/X) system and the second an X-band up/Ka-band down (X/Ka) system. For both systems, the LGA is omitted with the assumption that the spacecraft can recover from tumbling by use of onboard sensors and autonomy. Several assumptions are made for both the X/X and X/Ka systems: one HGA and connecting waveguide and redundant transmitters and transponders. A database is established that contains data for a variety of components, some of which are inherited from other projects, such as Cassini, Pluto Express, Mars Pathfinder (MPF), and Space Infrared Telescope Facility (SIRTF), while the remainder are from manufacturers' data for space components (see Appendix A). In Section II.C.1, we begin by presenting the X/X systems, followed by the X/Ka systems in Section II.C.2.

1. X/X RF Telecommunications Systems. A schematic of the X/X RF system is shown in Fig. 2. For the three data volumes, 0.1, 1.0, and 10.0 Gb/day, the major system components are an HGA, a diplexer, redundant small deep-space transponders (SDSTs), a redundant X-band HPA, hybrids, and a waveguide transfer switch (WTS). The physical characteristics for each of the above components are presented in Table 2. All of the hardware components are the same for the three data volumes except

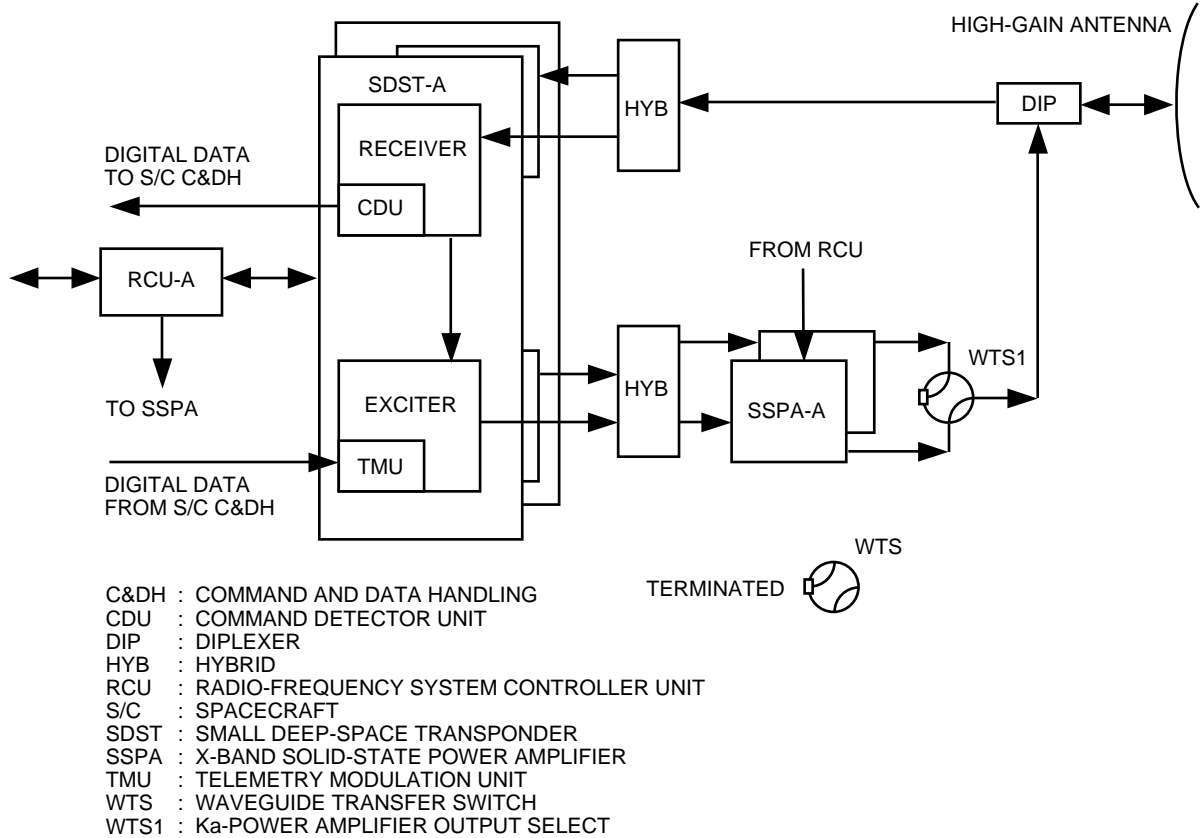


Fig. 2. X/X/ system design with no LGA.

Table 2. X/X system hardware description list (data volumes 0.1, 1.0, and 10.0 Gb/day).

No. of units	Data volume, Gb/day	Item	Unit mass, kg	Total mass, kg	Volume, cm ³	DC power, W
1	0.1	HGA, 1.0-m diameter	1.4	1.4	—	—
1	1.0	HGA, 1.4-m diameter	2.5	2.5	—	—
1	10.0	HGA, 2.0-m diameter	7.9	7.9	—	—
1	0.1, 1.0, 10.0	Diplexer	0.55	0.55	31 × 18 × 5.4	—
2	0.1	1.6-W X-band SSPA ^a	0.11	0.22	—	4.88
2	1.0	8.0-W X-band SSPA ^a	0.50	1.00	—	26.0
2	10.0	40-W TWTA	3.17	6.34	—	90.9
2	0.1, 1.0, 10.0	SDST	1.8	3.6	10 × 10 × 8	11
1	0.1, 1.0, 10.0	Waveguide switch	0.4	0.4	10 × 8 × 5.4	—
1	0.1, 1.0, 10.0	RFS control unit	1.5	1.5	18 × 10 × 2.5	3
2	0.1, 1.0, 10.0	Hybrid	0.1	0.2	5 × 5.6 × 2.5	—
1 lot	0.1, 1.0, 10.0	Waveguides/misc.	2.2	2.2	2.5 × 2.5 × 10	—
Total	0.1			10.0		18.9
	1.0			12.0		40.0
	10.0			22.7		104.9

^a The series of X-band SSPAs (1.6 and 8 W) is based on the JPL in-house design experience of the MPF 13-W SSPA.

for the HGA and the HPA. For 0.1 Gb/day, two 1.6-W X-band SSPAs are used, each weighing 0.11 kg and consuming 4.88 W. For 1.0 Gb/day, two 8-W X-band SSPAs are used, each weighing 0.5 kg and consuming 26.0 W. For 10.0 Gb/day, two 40-W X-band TWTAs (Mars Observer) are used, each weighing 3.17 kg and consuming 90.9 W. The three designs are based on HGAs of 1, 1.4, and 2.0 m in diameter, which have masses of 1.4, 2.5, and 7.9 kg, respectively. Also, the SDST includes the command data unit (CDU) and the telemetry modulation unit (TMU). The diplexer design is inherited from the MPF project; the WTS design is inherited from the Cassini project; and the radio-frequency system control unit (RCU) design is inherited from the Pluto Fast Flyby (PFF) study. The total mass and total power consumption for the three data volumes are shown in Table 2. The estimated relative costs for the three spacecraft terminal designs are shown in Table 3.

The uncertainty in these cost elements is not large, as many of the individual elements are either available off-the-shelf or in the midst of a mature development process (e.g., the SDST). Such uncertainty as exists is concentrated in the engineering or integration line items and may result in a 10- to 15-percent uncertainty in the total cost figure.

2. X/Ka RF Telecommunications Systems. A schematic of the X/Ka RF system is shown in Fig. 3. For the three data volumes, 0.1, 1.0, and 10.0 Gb/day, the major system components are an HGA, a filter, redundant SDSTs, a redundant Ka-band HPA, hybrids, and a WTS. The physical characteristics for each of the above components are shown in Table 4. The first two designs are based on the use of 1.0- and 1.4-m-diameter HGAs that weigh 1.4 and 2.5 kg, respectively, including a connecting waveguide. These two designs use redundant Ka-band SSPAs of different power levels, 0.4 W and 2.1 W for the data volumes of 0.1 and 1.0 Gb/day, respectively. The third design (10 Gb/day) is based on a 2.0-m-diameter HGA that weighs 7.9 kg and includes the connecting waveguide. Redundant 15-W TWTAs are used for HPAs; each weighs 3.44 kg and consumes 32 W. The TWTA design is inherited from the Cassini project.

Table 3. X/X system, no spare hardware and no LGA.

Description	0.1 Gb/day (1.6-W SSPA)	1.0 Gb/day (8-W SSPA)	10.0 Gb/day (40-W MO)
Cost (relative to 0.1-Gb/day case)	1.0	1.02	1.07
Mass, kg	10.0	12.0	22.7
Power, W	18.9	40.0	104.9

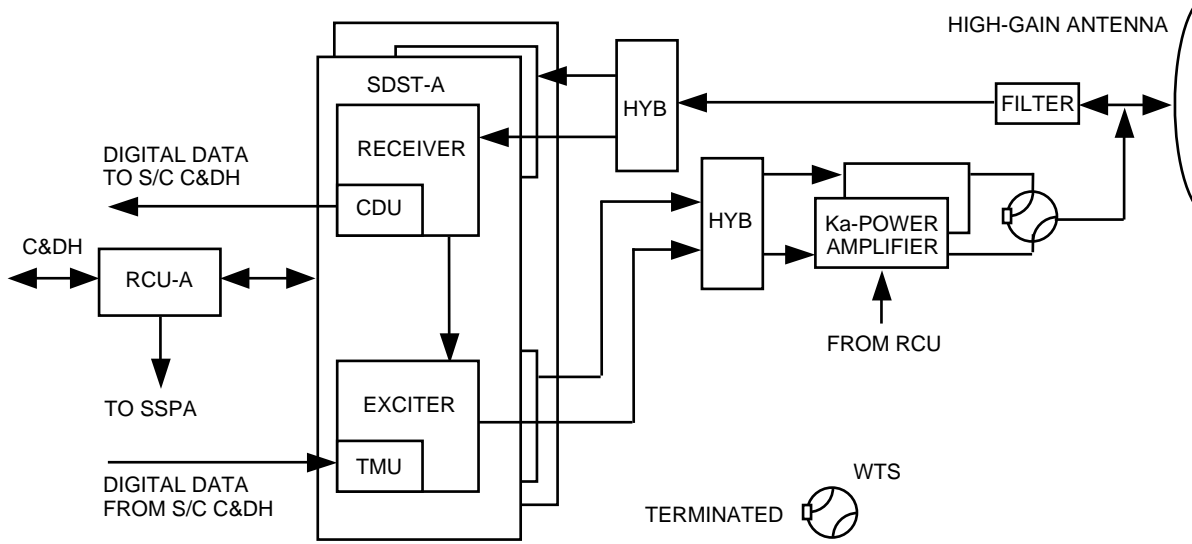


Fig. 3. X/Ka system hardware description list (data volumes 0.1, 1.0, and 10.0 Gb/day).

Also, the mass of the SDST includes the CDU and the TMU. The 1.4-m HGA design is identical to the SIRTf HGA, while the 2.0-m HGA and the RF RCU designs are inherited from the PFF study. The filter is the MGS project design. The WTS is a spare from the Cassini project. The total mass and total power consumption for the three system designs corresponding to the three data volumes are shown in Table 4. The estimated relative costs for the three spacecraft terminal designs are shown in Table 5.

The uncertainty in these cost elements is not large as, again, many of the individual elements are either available off-the-shelf or in the midst of a mature development process (e.g., the SDST). Such uncertainty as exists is concentrated in the engineering or integration line items, plus the Ka-band SSPA. The Ka-band SSPA element is only 20 percent of the total cost, so a probable uncertainty of 25 percent in that one item should not add more than 5 percent to the uncertainty of the total cost figure. The aggregate uncertainty remains on the order of from 10 to 15 percent of the total cost figure. Because many of the actual elements of the Ka-band and X-band terminals are common, the differential uncertainty of their costs should be small, perhaps from 5 to 10 percent of the total cost figure.

3. Alternative Ground Systems. In addition to the 34-m subnets of antennas, the DSN includes one subnet of 70-m antennas, usually allocated to missions with the greatest need for sensitivity, such as the current Galileo spacecraft. It is instructive to examine the effect of substituting these large 70-m antennas for the 34-m systems discussed above.

Table 4. X/Ka system hardware description list (data volumes 0.1, 1.0, and 10.0 Gb/day).

No. of units	Data volume, Gb/day	Item	Unit mass, kg	Total mass, kg	Volume, cm ³	DC power, W
1	0.1	HGA, 1.0-m diameter	1.4	1.4	—	—
1	1.0	HGA, 1.4-m diameter	2.5	2.5	—	—
1	10.0	HGA, 2.0-m diameter	7.9	7.9	—	—
1	0.1, 1.0, 10.0	Filter/dual-feed	0.55	0.55	31 × 18 × 5.4	—
2	0.1	0.4-W Ka-band SSPA	0.07	0.14	7.6 × 4.5 × 2.5	1.2
2	1.0	2.1-W Ka-band SSPA	0.15	0.30	9.4 × 8 × 2.5	11
2	10.0	15-W Ka-band TWTA	3.05	6.1	34 × 22 × 22	32
2	0.1, 1.0, 10.0	SDST	1.8	3.6	10 × 10 × 8	11
1	0.1, 1.0, 10.0	Waveguide switch	0.4	0.4	10 × 8 × 5.4	—
1	0.1, 1.0, 10.0	RFS control unit	1.5	1.5	18 × 10 × 2.5	3
2	0.1, 1.0, 10.0	Hybrid	0.1	0.2	5 × 5.6 × 2.5	—
1 lot	0.1, 1.0, 10.0	Waveguides/misc.	2.2	2.2	2.5 × 2.5 × 10	—
Total	0.1			10.0		15.2
	1.0			11.3		25.0
	10.0			22.5		46.0

Table 5. X/Ka system, no spare hardware, no LGA, and X/Ka feed.

Description	0.1 Gb/day (0.4-W SSPA)	1.0 Gb/day (2.1-W SSPA)	10.0 Gb/day (15-W Cassini)
Cost (relative to X/X 0.1-Gb/day case)	1.04	1.13	1.19
Mass, kg	10.0	11.3	22.5
Power, W	15.2	25.0	46.0

At X-band, the performance of the 70-m antennas is approximately 5.5-dB more sensitive (in G/T) than that of the 34-m antennas at the reference elevation angle and atmospheric conditions. Rather than work the details of redesigning and reestimating the link and flight terminal parameters specifically for the 70-m case, we chose instead to handle this 5.5 dB of additional performance as an offset from the designs already developed. The designs were constrained to use one of the three preselected antenna apertures in the data base, along with a suitable power amplifier. Thus, there may be some further optimization that could be performed. Table 6 shows the approximate flight terminal parameters for the 70-m antenna X-band case in comparison with those using the 34-m antenna.

At Ka-band, the large-aperture situation is less clear. There are significant technical challenges to making the 70-m antenna able to point effectively and to keeping it from degrading in performance under gravity or wind loading. Assuming that technology development efforts to adapt the 70-m antenna for Ka-band operation result in a 50-percent efficient antenna with a 50-percent reduction in gravity-loading effects, the net sensitivity of that 70-m antenna at Ka-band could be about 5.0 dB more than that of the 34-m antenna. An array of three 34-m antennas represents an alternative aperture with performance just slightly less than 5 dB above that of the single 34-m antenna. The Ka-band flight terminal parameters

should be approximately the same for either form of the larger ground configuration, and again were estimated as an offset to the designs just described. Table 7 shows the approximate flight terminal parameters for the 70-m antenna Ka-band case in comparison with those using the 34-m antenna.

As indicated by the tables, at a 10-Gb/day data volume, there can be an advantage of a 25- to 30-percent reduction in flight terminal mass and/or power associated with use of the larger ground aperture. This advantage declines to about 15 percent at 1 Gb/day and to only a few percent at a 0.1-Gb/day data volume. Also, this reduction is not without costs elsewhere, as the nominal price for operating the 70-m antenna is almost three times that of the smaller antennas. As will be seen in our follow-on article,⁴ if overall cost to NASA is the criterion of interest, the added cost of running the 70-m antenna for the required time span will override the cost savings associated with the reductions on the spacecraft.

Table 6. X-band flight terminal parameters with 70-m reception.

Item	0.1 Gb/day		1.0 Gb/day		10.0 Gb/day	
	70-m	34-m	70-m	34-m	70-m	34-m
Antenna, m	1.0	1.0	1.0	1.4	2.0	2.0
RF power, W	0.5	1.6	4.5	8.0	11.0	40.0
DC power, W	15.4	18.9	28	40	58	105
Mass, kg	10.0	10.0	10.3	12.0	18.4	22.7
Recurring, relative to a flight-unit X/X 0.1-Gb/day case	0.7	0.7	0.7	0.7	0.8	0.8

Table 7. Ka-band flight terminal parameters with 70-m reception.

Item	0.1 Gb/day		1.0 Gb/day		10.0 Gb/day	
	70-m	34-m	70-m	34-m	70-m	34-m
Antenna, m	1.0	1.0	1.0	1.4	1.4	2.0
RF power, W	0.13	0.4	1.3	2.1	10	15
DC power, W	14.5	15.2	19.5	25	36	46
Mass, kg	10.0	10.0	10.1	11.3	17.1	22.5
Recurring, relative to a flight-unit X/X 0.1-Gb/day case	0.7	0.7	0.7	0.8	0.8	0.8

III. Optical Communications

In this part of the article, use of optical frequencies for communication between a spacecraft at Mars and Earth are discussed in two segments. Section III.A discusses the ground receiver conceptual design and performance characteristics. The flight terminal conceptual design and characteristics are discussed in Section III.B.

⁴C. Chen et al., op cit.

A. Ground Optical Terminal and Network

The overall design of the ground optical telecommunications terminal is based upon a design concept that consists of a receiving system, a transmit system, data processing and support electronics, and station facilities. Four network concepts were examined, using this ground optical telecommunications terminal as a building block. They ranged from the worldwide seven-station linearly dispersed optical subnet (LDOS) concept [1] to one-, two-, or three-station configurations in the continental U.S.

The receiving system consists of a 10-m nondiffraction-limited segmented primary mirror with a monolithic secondary in a Cassegrain configuration, as shown in Fig. 4. A lower-cost 3.5-m station also was considered.

A detailed description of the ground terminal is given in Appendix B. Costing results, relative to a flight unit of the X/X 0.1-Gb/Day case, for development and operations of each of the four alternatives are presented in Table 8. These estimates are considered to be rough, with a probable uncertainty range of +30 to -0 percent.

B. Space Terminal

The spaceborne terminal consists of three main subsystems. These are the acquisition, tracking, and pointing subsystem; the transmitter subsystem; and the transmit/receive aperture and associated optics. Each of these subsystems is described below.

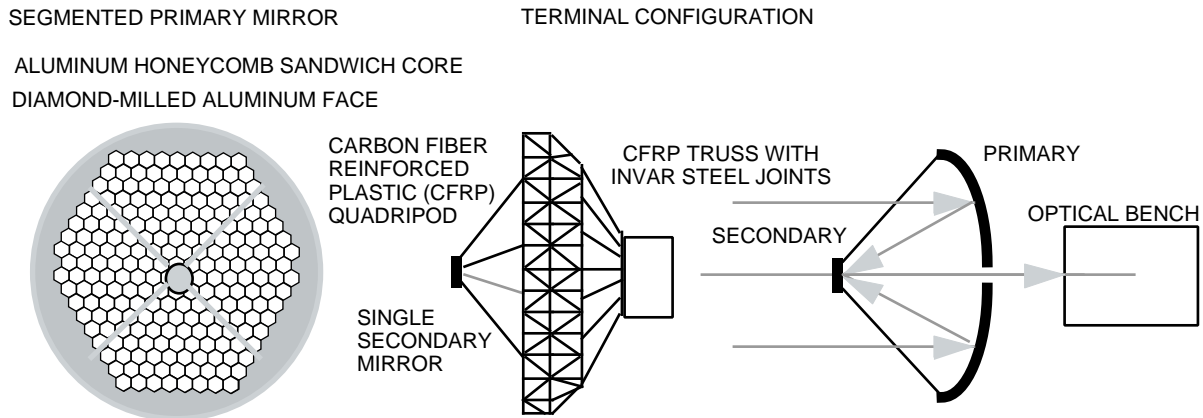


Fig. 4. Schematic of a 10-m receiver.

Table 8. Optical ground network normalized cost estimates relative to a flight-unit X/X 0.1-Gb/day case.

Net configuration	10-m-aperture diameter		3.5-m-aperture diameter	
	Implementation	Annual operations	Implementation	Annual operations
Single-station	3	0.2	2	0.2
Two-station	6	0.3	4	0.3
Three-station	9	0.5	6	0.5
Seven-station	19	0.8	12	0.8

1. Acquisition, Tracking, and Pointing. Prior to establishing the communications link, the space and ground terminals need to perform mutual acquisition of each other’s signal. The acquisition process involves the following steps: (1) determination of Earth position and orientation of the spacecraft to position the Earth receiver station within the spacecraft terminal’s field of view; (2) identification of the position of the Earth receiver station to better than 5 to 10 percent of the downlink signal beamwidth; and (3) determination of the angle offset (point-ahead) of the downlink beam such that the signal from the spacecraft is received by the ground station. The two basic acquisition and tracking approaches considered were (1) active beacon-assisted acquisition and tracking and (2) Earth-image-based extended-source acquisition and tracking. Extended-source tracking using the sunlit Earth is a viable option for a Mars mission and was selected for the present study. However, for the Mars mission (2.7 AU), tracking an uplink laser beacon also is a viable option. It should be considered in future studies as well since it eliminates the need for a dedicated flight processor. Details of the acquisition and tracking process are given in [7].

2. Flight Terminal Conceptual Design. The emphasis of the flight terminal conceptual design was on reduced mass and power consumption. Briefly, the terminal uses internal steering elements for beam-pointing stabilization and a combination of platform isolation and active optical feedback of sunlit Earth images for jitter compensation. Also, the terminal uses precision two-way ranging to derive necessary navigation variables and dual-redundant active optical elements for improved system reliability.

A block diagram of the optical transceiver and its interface with the spacecraft along with a schematic diagram of the hardware are presented in Figs. 5 and 6, respectively. Redundant units on the transceiver are shown as shaded boxes. The spaceborne terminal consists of a single receive-transmit telescope where receive/transmit isolation is obtained by proper filtering of the diverse wavelengths involved. The optical train consists of two main arms: a transmit arm that originates at the laser transmitter and extends to the telescope, and a receive arm including data reception and acquisition and tracking that originates at the telescope and terminates at the focal plane detectors. The two arms overlap each other during part of their paths. This ensures that the transmit beam is pointed at the ground-based beacon (which may be the sun-illuminated Earth). Redundant laser transmitters are diode-pumped Nd:YLF lasers (at 1054 nm) that provide the peak powers that are necessary for communications from the range of 2.7 AU. To reduce system mass, where possible, the optical train of the transceiver was designed based on block-coupled optics. The focal plane of the receive/transmit telescope was assumed to consist of two avalanche photodiode (APD) data detectors and two active-pixel-sensor (APS) detectors for acquisition and tracking, all tightly packaged. In this design, a zoom lens was incorporated into the optical train to change the image size on the focal plane. As shown in Fig. 5, the transceiver package includes a laser-communication control unit (LCU). The LCU is a processor (e.g., Motorola’s MOPS6000) in contact, through the spacecraft bus, with the spacecraft’s command and data handling (C&DH) unit. Its functions are to process acquisition and tracking data (e.g., for extended-source tracking), transmit data, and provide other necessary control features.

Link parameters for the three data volumes of 0.1, 1.0, and 10.0 Gb/day are summarized in Table 9. The detailed link control table for the 10-Gb/day case appears in Table B-1 of Appendix B. These were obtained using JPL’s optical communication link analysis (OPTI) program. The analysis assumed a maximum range of 2.7 AU; a required bit-error rate of 1×10^{-5} (with coding); an atmospheric transmission factor of 0.45 at 1054 nm, corresponding to an elevation angle of 30 deg; a single 10-m photon-bucket receiver located in Hawaii at a 4.2-km altitude; daytime as well as nighttime ground reception; and a link margin of 2.5 dB. Analysis indicated that a 2.3-W (average power) laser transmitter in conjunction with a 35-cm transmit aperture will provide a data rate of 500 kbps and a data volume of 10 Gb/day to a single 10-m station. The required aperture size and laser output power decrease to 10 cm and 0.45 W, respectively, for a daily communication volume of 0.1 Gb.

Two alternative configurations, each capable of 10 Gb/day, also are shown in Table 9. Both of these require the use of three separate ground terminals distributed about the Earth, much like the current

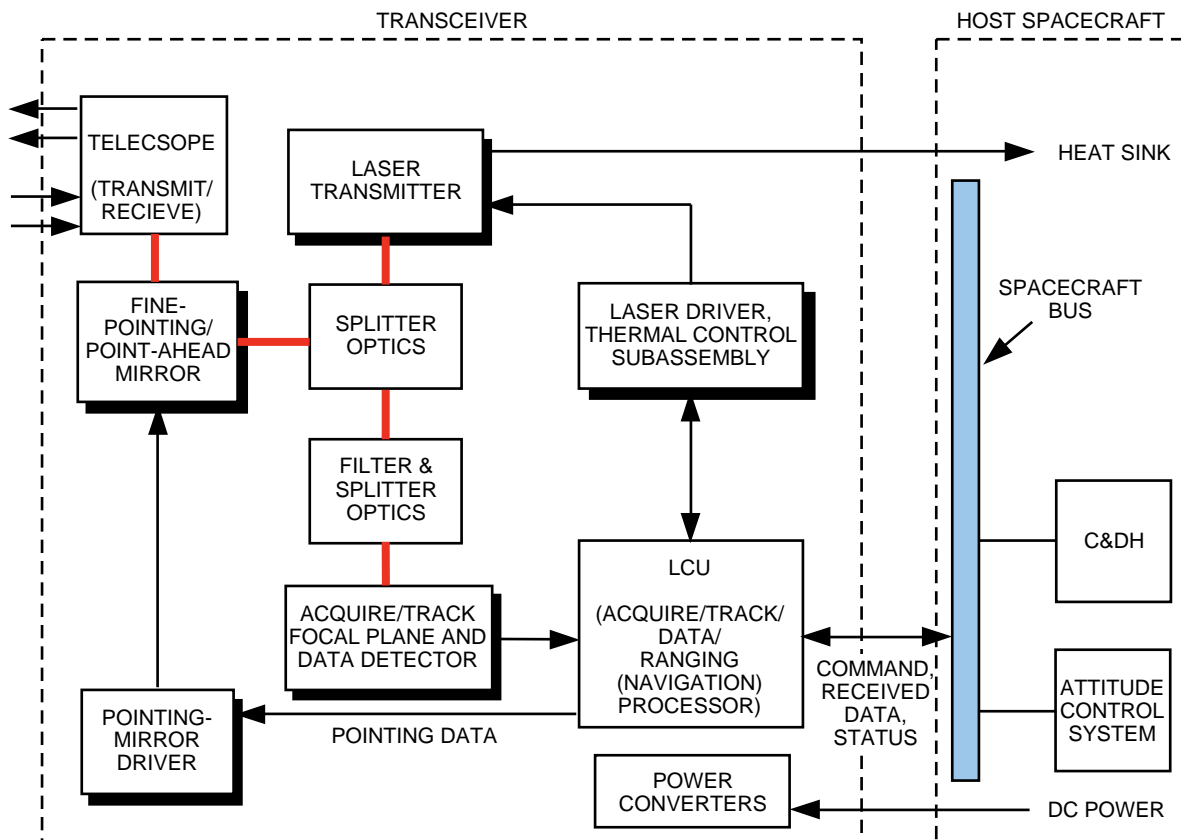


Fig. 5. The optical transceiver and its spacecraft interface.

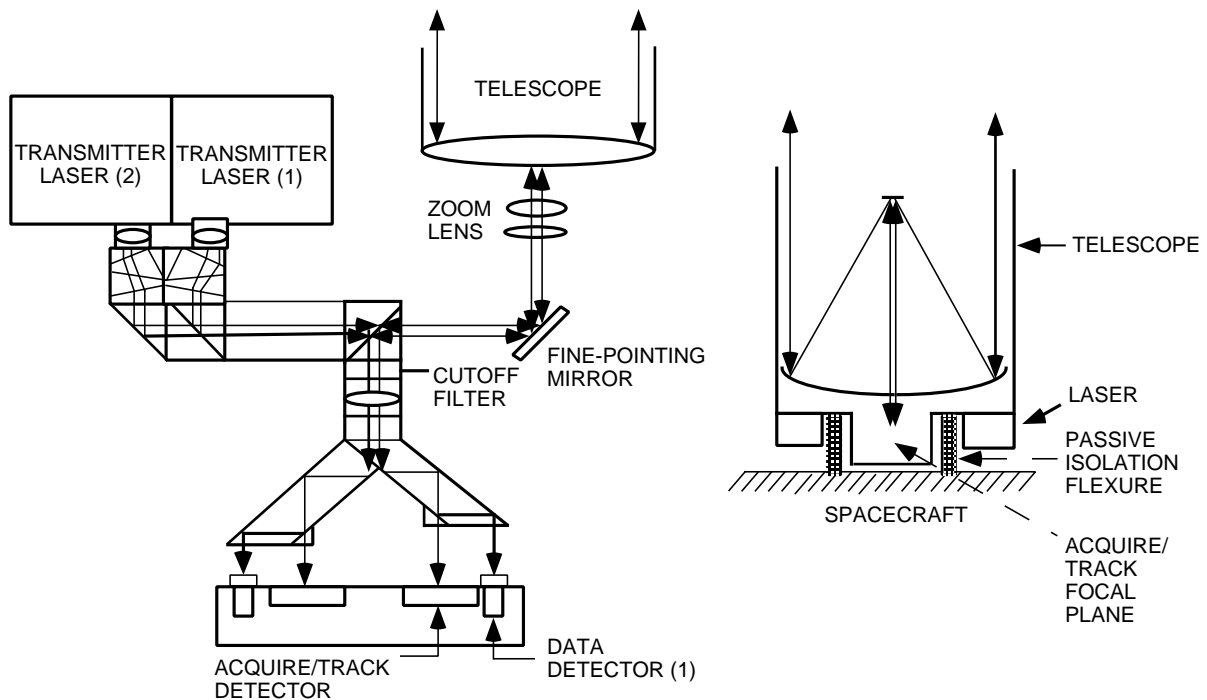


Fig. 6. Schematic of the transceiver.

Table 9. Link parameter summary.^a

Item	Data volume, Gb/day (station)				
	0.1 (single 10-m)	1.0 (single 10-m)	10.0 (single 10-m)	10.0 (three 10-m)	10.0 (three 3.5-m)
Data rate, kbps	15	50	500	200	200
Transmit telescope diameter, m	0.1	0.15	0.35	0.25	0.35
Average output power, W	0.45	0.69	2.3	1.35	2.3
Ground network contact, h/day	2.1	8.5	8.1	19	19
Beamwidth, μ rad	17.5	12	4.0	8	4.0

^a Assuming a transmit laser wavelength of 1054 nm, a link distance of 2.7 AU, a ground receiver diameter as noted, a required BER (uncoded) of 10^{-5} , an atmospheric transmission factor of 0.45 (at a 30-deg elevation angle), and a link margin of 2.5 dB. The data rate was adjusted upward (by 40 percent) to compensate for probabilistic weather unavailability.

microwave DSN, in order to compensate for reduction in spacecraft capability (i.e., to 1.35 W in 25 cm) or ground terminal size (to 3.5 m). Neither alternative is cost effective in its current form, largely due to the investment needed in the ground terminals. However, either of the three-station configurations offers the potential of telecommunications contact at any time (weather permitting). And, if for some external reason the flight terminal size, mass, and power are more important than end-to-end costs, then the greater ground capability with the three 10-m sites will permit that trade to occur.

A high-order ($M = 256$ and 512) pulse position modulation (PPM) format was selected for modulation of the diode-pumped solid-state laser. PPM involves translating a data word (string of data bits) into the position in time of a laser pulse, and vice versa. Advantages of a high-order PPM format are (1) increased direct detection sensitivities and (2) substantial rejection of background light via temporal filtering associated with short pulse (10-ns-level) integration times [6].

Reed–Solomon data coding was assumed in the analysis to improve system performance by requiring fewer detected photons per information bit be received in order to attain a prescribed decoded bit-error rate (a BER of 10^{-5}). With a coding rate of $3/4$ and with $M = 512$, the required BER was set equal to 4×10^{-2} in the link-control table, and the required data rate was adjusted accordingly, with a multiplier factor of $4/3$.

The procedure for calculating the expected data volume, the required number of ground stations to support those data volumes, and the link-control table uncertainties are described in Appendix C.

3. Mass, Power, Size, and Relative Cost Estimates. Mass, power, size, and relative cost estimates for the spaceborne terminal are summarized in Table 10. To calculate mass and power consumption, the system was partitioned into subsystems and then into individual components. A mass and power consumption value was allocated to each component and/or subsystem. Appendix D presents the details of the mass and power estimation for the 25-cm, 1.35-W terminal. Probable error and redundancy factors are included as applicable.

Cost estimates for the first flight unit were calculated in the same manner. A major (>50-percent) reduction in the cost of producing subsequent units is anticipated. Costing assumptions were that all

Table 10. Mass, power, size, and relative cost summary.

Item	Telescope diameter (transmitter power)			
	10 cm (0.45 W)	15 cm (0.69 W)	25 cm (1.35 W)	35 cm (2.3 W)
Mass, kg	6.4 ± 0.9	7.4 ± 1.2	9.0 ± 1.2	12.1 ± 1.7
Laser subsystem (redundant)	2.1	2.5	3.1	4.4
Transmit/receive aperture	1.3	1.9	2.8	4.6
Acquire/track/pointing/communications subsystem (redundant)	0.7	0.7	0.7	0.7
Thermal/mechanical	0.8	0.8	0.9	0.9
Other (processor, etc.)	1.5	1.5	1.5	1.5
Power, W	19.9 ± 7	22.8 ± 4	30 ± 6	44.6 ± 4.6
Laser subsystem	4.7	7.2	13.7	26.2
Transmit/receive aperture	0.5	0.5	0.5	0.5
Acquire/track/communications subsystem	3.6	3.6	3.6	3.6
Thermal/mechanical	0.5	0.5	0.5	0.5
Other (processor, etc.)	10.6	11.0	12.0	13.8
First flight-unit cost, relative to X/X 0.1-Gb/day case	1.2	1.2	1.3	1.3
Second flight-unit cost, relative to X/X 0.1-Gb/day case	0.4	0.4	0.5	0.5
Size, cm ³	$15 \times 15 \times 30$	$20 \times 20 \times 40$	$30 \times 30 \times 45$	$30 \times 35 \times 45$
Data volume capability, Gb/day	0.1	1.0	10.0	10.0

costs be in constant 1995 dollars and that there be a technology freeze date of December 1996. Cost includes system engineering; flight hardware and software development; ground support equipment (for testing); system integration and test support; mission operations planning support; reliability engineering and quality assurance; and management. Deliverables are development and breadboarding of critical components, namely, the acquisition and tracking focal plane and lasers; one flight unit plus documentation; and two sets of ground support equipment (one set delivered to the launch site). The development cycle is 3 years from start to launch.

Understanding the uncertainty in these estimated cost figures is hard. The uncertainty itself is not embedded within the specific numbers, but is associated with the assumptions behind them and, hence, with surprises, i.e., the unknowable. Some confidence in the estimated cost value is gained through the general confirmation by the model values for the first-article costs. Hence, it seems reasonable to believe that the uncertainty in the estimates generally is no larger than that ascribed to the models, or on the order of 20 percent. It should be recognized, however, that some surprises may lurk in the details of providing the metric function for navigation, replacing the RF coherent Doppler that no longer would be available. This is an area unexplored in the current study.

For the other flight terminals, the development cost for each terminal is nearly the same as for the 25-cm-aperture terminal. The only cost reduction area is in the laser transmitter. Due to a lower laser power requirement, a lower number of space-qualified pump diode lasers are needed. That will result in a lower overall cost of the subsystem. Within the range of required telescope diameters for this study (for different missions), the cost of optics (telescope, etc.) development remained essentially unchanged.

In conclusion, two alternative options are available for the design of the flight optical communication terminal: With a network of three 3.5-m telescopes (or a single 10-m telescope), the burden (higher terminal mass and power consumption) is shifted to the spacecraft side, while with a network of three 10-m telescopes, the burden (higher ground network cost) is shifted to the ground side.

IV. Considering Other Destinations

The initial formulation of the ACBS included three separate destinations: one at Mars to serve as an archetype for the nearby planetary targets; one at Neptune, representing the far outer planets; and one in the Earth–Luna neighborhood. Our expectation was that these three point designs would serve as anchors for consideration of arbitrary targets within the solar system. Having done the Mars point designs and initiated an extrapolation to the Neptune situation, it has become apparent that most of the issues there have been handled within the Mars context and that the design concepts worked for Mars, suitably adjusted, can serve for a variety of destinations.

The range between the spacecraft and Earth has a dominant effect on the ability to communicate, as the received signal strength falls off inversely proportional to the square of the distance traveled. Switching a communications link designed for the Mars–Earth service (at 2.7 AU) to operate at Neptune (at 30 AU) changes the signal power received at Earth by a factor of 0.008. And to the first order, the data rate capability of that link is changed by the same factor. Additionally, some nonlinear effects that are dependent upon absolute signal level will tend to reduce further the data rate capability at reduced signal levels.

To evaluate the impact of these nonlinearities, actual link performance was calculated for the use of the Mars-design flight terminals at Neptune range. For the optical systems, the predicted performance was found to match closely that as scaled by the range-factor alone. For the RF systems, however, the decrease in total received power causes difficulty in obtaining an adequate phase-coherent reference for low-loss detection. Some system design changes are needed, and for the highest (i.e., 80-Mb/day) data volume, use of suppressed-carrier modulation is sufficient. At the lower data volumes, it is also necessary to use a (much) narrower bandwidth in phase tracking the (reconstructed) suppressed-carrier signal. These capabilities are present in the DSN today and are utilized in reception of the Galileo signals. For use of the narrowed bandwidth at the ground, the onboard oscillator must be supplemented by a precision oscillator with low phase noise. A known oscillator of adequate performance considered for Near-Earth Asteroid Rendezvous (NEAR) spacecraft would add 0.3 kg of mass and require 1.6 W of power for a redundant unit.⁵ Given that such an oscillator is added to the flight units for 8 and 0.8 Mb/day, no other changes to the downlink signal are needed. A variety of alternative solutions is possible, including other modulation schemes, e.g., multiple-frequency shift keying (MFSK), or other oscillator designs, or simply use of increased downlink power and shorter contact times. A full search for the best solution is beyond the scope of the present study.

A long communication range to the outer planets also means long round-trip light times for signal transmission. When automatic repeat is used for error control on the links, the extremely long delay time could require added onboard storage and will complicate the accounting and control algorithms needed to ensure successful transfer.

Another complicating factor is the long flight time associated with the trajectories to the outer planets. A long flight before the start of mission data acquisition means a requirement for long lifetimes for onboard devices and perhaps the addition of redundancy to ensure those lifetimes. Trajectories to the outer planets are very likely to include a gravity assist at Jupiter, saving fuel but encountering high radiation in the process. Again, there are added requirements on the design of devices for a high-radiation environment.

⁵ G. E. Wood, personal communication, Jet Propulsion Laboratory, Pasadena, California, December 15, 1994.

These are messy issues that will add to the mass and cost of the telecommunications system but are beyond the scope of the present study.

When one considers the alternative of nearby destinations (closer than Mars), the limiting factor becomes not signal strength but actual rate limits on the data-handling equipment. At a range of 0.1 AU, the signal-strength limit is of the order of 3 Mbps for the smallest of the links considered for Mars. Current rate limits for RF reception and capture in the DSN are in the neighborhood of a few Mbps, although equipment being installed for orbiting very long baseline interferometry (VLBI) support will raise that to 144 Mbps on a new 11-m subnet. Transmission rates to JPL are lower, limited by cost of the commercial communications bandwidth, but shipment of recorded instrumentation tapes offers a nonreal-time alternative. If these constraints are released, available RF bandwidth offers another limit, which is a few tens of Mbps or a few hundreds of Mbps, depending upon which service allocation is being considered. Different limits apply to the optical channel, some related to laser physics and some to costs of data management and transport. A full comparison of RF and optical communications at close-in ranges is a complex subject that is outside the scope of the current study.

The telecommunications terminal on board a spacecraft depends upon other critical spacecraft resources, among which are power and available mass (as constrained by transportation). Both of these have economic aspects that change significantly depending upon the destination. The cross-impact of these economic factors upon the telecommunications function is explored via the combined metrics, which will be presented in our follow-on article.⁶ Numerical values used consider Neptune as the alternate destination.

V. Summary of Results and Concluding Observations

Comparison of the results for the three Mars telecommunications systems and for the three data volumes is presented in Table 11 and Figs. 7 through 9. Nominal cost values for the flight terminals are those estimated via the design process described in the preceding sections. This is a subset of the configurations examined and described earlier. This subset is constrained to use a single “standard” ground terminal for each of the communications bands, so that the variation with data volume appears in the same way in downlink power and directivity for all three bands. That ground terminal currently is in place for X-band. Some implementation and ground system investment is required for either Ka-band or optical frequencies.

Several general observations can be made based on Table 11 and the derived figures:

- (1) Optical flight terminals exhibit uniformly lower mass than does the RF, ranging from 65 percent at 0.1 Gb/day downward to 55 percent at 10 Gb/day, when compared with either RF terminal. The masses of the two RF terminals were seen to be approximately equal.
- (2) Ka-band requires lower power than does X-band, ranging from 80 percent at 0.1 Gb/day downward to 40 percent at 10 Gb/day. Optical frequencies consume slightly less power than does Ka-band, except at the lowest data volume. At 0.1 Gb/day, the optical power requirement is dominated by the overhead of the acquisition-tracking subsystem and is approximately equal to the X-band.
- (3) The costs of flight unit number 1 are roughly comparable for the X-band, Ka-band, and optical frequencies. They increase gradually with data volume, and decrease with technological readiness. Uncertainty in the costs (not shown) also decreases with technological readiness. The cost of flight unit number 2 is modestly lower than unit number 1 for the RF terminals and is believed to be markedly lower for the optical frequencies.

⁶ C. Chen et al., *op cit*.

Table 11. Comparison of the Mars spacecraft communication subsystems at different data volumes.

Data volume, Gb/day	Communication band	Mass, kg	DC power, W	Relative cost (first unit) ^a	Relative cost (second unit) ^a
0.1	X-band	10.1	18.9	1.0	0.7
	Ka-band	10.0	15.2	1.0	0.7
	Optical	6.4	19.9	1.2	0.5
1.0	X-band	12.0	40.0	1.0	0.7
	Ka-band	11.3	25.0	1.1	0.7
	Optical	7.4	22.8	1.3	0.5
10.0	X-band	22.7	104.9	1.0	0.7
	Ka-band	22.5	46.0	1.2	0.8
	Optical	12.1	44.6	1.3	0.5

^a The cost is normalized by the cost of the first-unit X/X 0.1-Gb/day case.

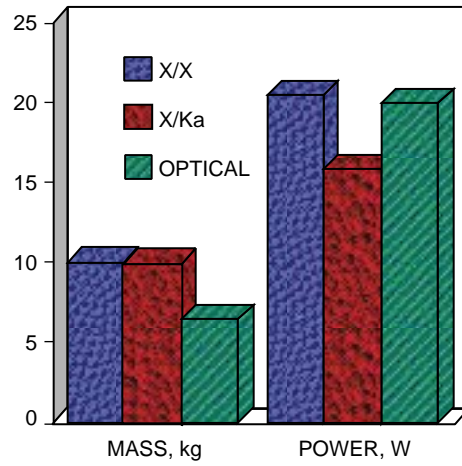


Fig. 7. Spacecraft mass and power comparison (0.1 Gb/day).

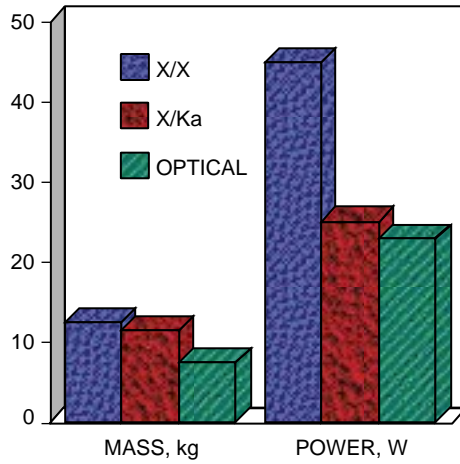


Fig. 8. Spacecraft mass and power comparison (1.0 Gb/day).

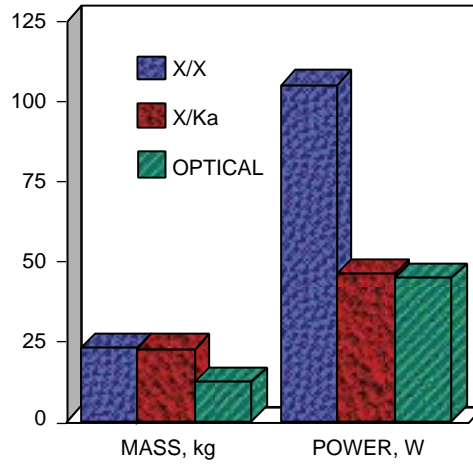


Fig. 9. Spacecraft mass and power comparison (10.0 Gb/day).

To obtain the value associated with the higher frequencies for the flight terminal end of the links requires an investment in ground-based facilities and perhaps an attitude change on the part of flight mission operations. Return of the specified data volumes requires only that a single ground site be available for collection of the data, as long as the data can be buffered on the spacecraft between contact times. However, in the past, missions have been able to schedule their contact times constrained only by spacecraft events and not by Earth receive time. This can be provided at the new frequencies but at a higher investment cost, as shown in Table 12, where investment cost is normalized by the reference cost of a first X/X flight unit at 0.1 Gb/day. For optical frequencies, the greater impact of weather requires diversity reception for the high availability coverage.

Table 12. Normalized cost of a ground facility for X-, Ka-, and optical bands.

Ground network configuration	X-band	Ka-band	Optical (70-percent availability)	Optical (high availability)
Single site	—	0.05	3	9
Worldwide	—	0.8	9	19

The telecommunications subsystems designed for Mars could be employed at Neptune with a reduction by a factor of 0.008 in the returned data volume. No changes appear to be needed to the optical subsystem designs. For the RF systems, the addition of a low-phase-noise oscillator would, in general, be required. Such an oscillator would add relatively small mass, power, and cost, but would not change the general conclusions in any appreciable way.

It is worth noting that trade-offs can be made between mass and power at any given data volume, depending upon what is in a specific mission design. Reduction in flight terminal mass can be achieved by decreasing the selected transmitting aperture size, but this increases the required power if the data volume is to be held constant. Similarly, a reduction in selected power consumption can be achieved through an increase in the transmitting aperture, provided it fits within the space allotted on the launch vehicle. Also, both mass and power can be decreased if one is willing and able to transfer added requirements to the ground receiving system.

At this stage of the study, a number of difficult issues remain that continue to obscure the application of the displayed results for any specific real situation. These issues are identified in the text of this article and in general represent topics that were set aside to constrain the study effort to a manageable level. Included among these are variations in technological maturity, variations in the metric functions for navigation, and the assumption of no low-gain emergency communications. Some additional studies and continued technology development for both Ka-band and the optical frequencies should help clarify matters as well as improve the viability of these bands. In the meantime, the designers of any planned operational deep-space communications system should examine the trade space with their own constraints and requirements.

Acknowledgments

The authors are indebted to C. Edwards, P. Estabrook, R. Mathison, F. Pollara, C. Stelzried, L. Swanson, and many others at JPL for stimulating and fruitful discussions.

References

- [1] K. Shaik, D. Wonica, and M. Wilhelm, "Optical Networks for Earth-Space Communications and Their Performance," *SPIE Proceedings, Free-Space Laser Communication Technologies VI*, vol. 2135, pp. 156–176, 1994.
- [2] W. M. Owen, Jr. "Telescope Pointing for GOPEX," *The Telecommunications and Data Acquisition Progress Report 42-114, April-June 1993*, Jet Propulsion Laboratory, Pasadena, California, pp. 230–233, August 15, 1993.
- [3] J. Yu and M. Shao, "Galileo Optical Experiment (GOPEX) Optical Train: Design and Validation at the Table Mountain Facility," *The Telecommunications and Data Acquisition Progress Report 42-114, April-June 1993*, Jet Propulsion Laboratory, Pasadena, California, pp. 236–241, August 15, 1993.
- [4] K. Wilson, "An Overview of the GOLD Experiment Between the ETS-VI Satellite and the Table Mountain Facility," *The Telecommunications and Data Acquisition Progress Report 42-124, October-December 1995*, Jet Propulsion Laboratory, Pasadena, California, pp. 8–19, February 15, 1996.
http://tda.jpl.nasa.gov/tda/progress_report/42-124/124I.pdf
- [5] M. Jeganathan, K. Wilson, and J. R. Lesh "Preliminary Analysis of Fluctuations in the Received Uplink-Beacon-Power Data Obtained From GOLD Experiments," *The Telecommunications and Data Acquisition Progress Report 42-124, October-December 1995*, Jet Propulsion Laboratory, Pasadena, California, pp. 20–32, February 15, 1996.
http://tda.jpl.nasa.gov/tda/progress_report/42-124/124J.pdf
- [6] R. M. Gagliardi and S. Karp, *Optical Communications*, New York: J. Wiley & Sons, 1976.
- [7] H. Hemmati, K. Wilson, M. Sue, D. Rascoe, F. Lansing, L. Harcke, M. Wilhelm, and C. Chen, "Comparative Study of Optical and RF Communication Systems for a Mars Mission," *SPIE Proceedings, Free Space Laser Communication Technology VIII*, vol. 2699, pp. 146–164, January 1996.
- [8] K. Pausch, *3.0/3.5-Meter Telescope*, Vertex Antennentechnik, Baumstr. 50, D-47198 Duisburg, Germany, January 24, 1996.
- [9] J. R. Lesh, "Technology, Data Bases and System Analysis for Space-to-Ground Optical Communications," Invited Paper 13.5, *Proceedings of Milcom 95*, San Diego, California, pp. 415–419, November 5–8, 1995.
- [10] S. G. Lambert and W. L. Casey, *Laser Communications in Space*, Boston, Massachusetts: Artech House, 1995.
- [11] E. Korevaar, R. J. Hofmeister, J. Schuster, C. Chow-Miller, P. Adhikari, H. Hakakha, D. Cuthbert, and R. Ruigrock, "Design of Satellite Terminal for BMDO Lasercom Technology Demonstration," *Proceedings of SPIE Photonics West*, vol. 2381, San Jose, California, pp. 60–71, February 7–8, 1995.
- [12] Y. Arimoto, M. Toyoshima, M. Toyoda, T. Takahashi, M. Shikatani, and K. Araki, "Preliminary Result on Laser Communication Experiment Using ETS-VI," *Proceedings of SPIE Photonics West*, vol. 2381, San Jose, California, pp. 151–158, February 7–8, 1995.
- [13] T. Araki, S. Nakameri, Y. Hisada, and T. Fukuda, "Present and Future of Optical Intersatellite Communications Research at NASDA," *Proceedings of SPIE OE/Lase 94*, vol. 2123, Los Angeles, California, pp. 2–13, January 26–28, 1994.

- [14] A. F. Popescu and B. Furch, “Status of the European Developments for Laser Intersatellite Communications,” *Proceedings of SPIE OE/Lase 93*, vol. 1866, Los Angeles, California, pp. 10–20, January 20–21, 1993.

Appendix A

Database of Antennas and Power Amplifiers

The antenna designs are based on using advanced composite material, graphite epoxy. The antenna size is limited by the launch vehicle diameter, which is about 2 m. The cost estimates are based on Boeing’s design and fabrication (see Table A-1).

The solid-state power amplifier (SSPA) designs for X-band and Ka-band are presented in Tables A-2 and A-3. The mass, cost, and power consumption are inherited from the designs for Cassini, Mars Pathfinder, Pluto Express, and Mars Global Surveyor. The parameters and heritage of the traveling-wave power amplifiers are presented in Tables A-4 and A-5.

Table A-1. Antenna mass based on the Pluto advanced composite antenna (Boeing).

Diameter, m	Mass, kg
0.5	0.6
1.0	1.4
1.4	2.5
2.0	7.9

Table A-2. X-band solid-state power amplifiers’ mass and power consumption.

SSPA RF power, W	SSPA DC power, W	Power supply mass, g	SSPA mass, g	Total mass, g
0.25	0.6	35	35	70
0.5	1.4	35	35	70
1.0	3.2	50	40	90
2.0	6.0	75	45	120
5.0	15.0	125	45	170
8.0	26.0	150	350	500
13.0	56.0	200	1500	1700
20.0	80.0	250	1500	1750

Table A-3. Ka-band solid-state power amplifiers' mass and power consumption.

SSPA RF power, W	SSPA DC power, W	Power supply mass, g	SSPA mass, g	Total mass, g
0.25	0.8	35	30	65
0.5	1.4	35	35	70
1.5	6.0	75	40	115
2.6	13.0	125	45	170
3.5	18.0	125	50	175

Table A-4. X-band traveling-wave tube amplifier designs.

Frequency, GHz	Power output, W	Model no.		Efficiency, percent		Weight, kg		Program
		TWT	EPC	TWT	EPC	TWT	EPC	
7.2–8.4	40	3618-9	—	50	—	0.77	—	MO
7.2–8.4	50	3618-10	1669H	50	88	0.77	2.40	BRASILSAT, SUPERBIRD
7.2–8.4	50–60	3618-11	—	60	—	0.80	—	Development

Table A-5. Ka-band helix traveling-wave tube amplifier designs.

Frequency, GHz	Power output, W	Model no.		Efficiency, percent		Weight, kg		Status
		TWT	EPC	TWT	EPC	TWT	EPC	
22/32	10	950H	—	33	—	0.95	—	Qualified
31.8–32.3	10	955H	—	43	81	0.86	2.70	Development
32	15	—	—	46	—	0.8	2.25	Cassini

Appendix B

Optical Communication Ground Optical Terminal and Network

Details of the ground receiver telescope and a network of these telescopes are discussed here. This appendix includes a discussion of the ground telescope conceptual design and operation principles and cost estimates for the ground station(s). Uplink transmitter requirements and specifications are discussed in this appendix as well. A more detailed discussion of the ground receiver is provided in a JPL internal document.⁷

I. Receiving System

The telescope is mounted on an azimuth-elevation gimbal mount and is housed in a collapsible enclosure (dome). The receiving system also includes the optical bench, consisting of beam-reducing optics, a fast-steering mirror, a spectral filter, and tracking and communications detectors. System and component performance requirements were previously reported in [1].

The receiving aperture utilizes a segmented primary containing numerous segments for a total effective aperture of 10 m. Both the segments and the aperture are hexagonal in shape. The individual panels are actively controlled and are mounted on ball screw actuators. The primary support structure consists of an erectable truss manufactured from carbon fiber reinforced plastic (CFRP). The secondary mirror consists of a 1-m monolithic primary mounted on a CFRP quadripod. Figure B-1 describes the panel mounting configuration for the primary, including the active control system.

Analysis of the downlink performance of this receiving system in conjunction with various spacecraft terminals has been performed using the optical communication link analysis (OPTI) software. Suitable flight spacecraft terminals, to be described later, are shown to be easily capable of providing the desired data volumes. An example of the detailed link parameters produced by the OPTI program appears in Tables B-1 and B-2.

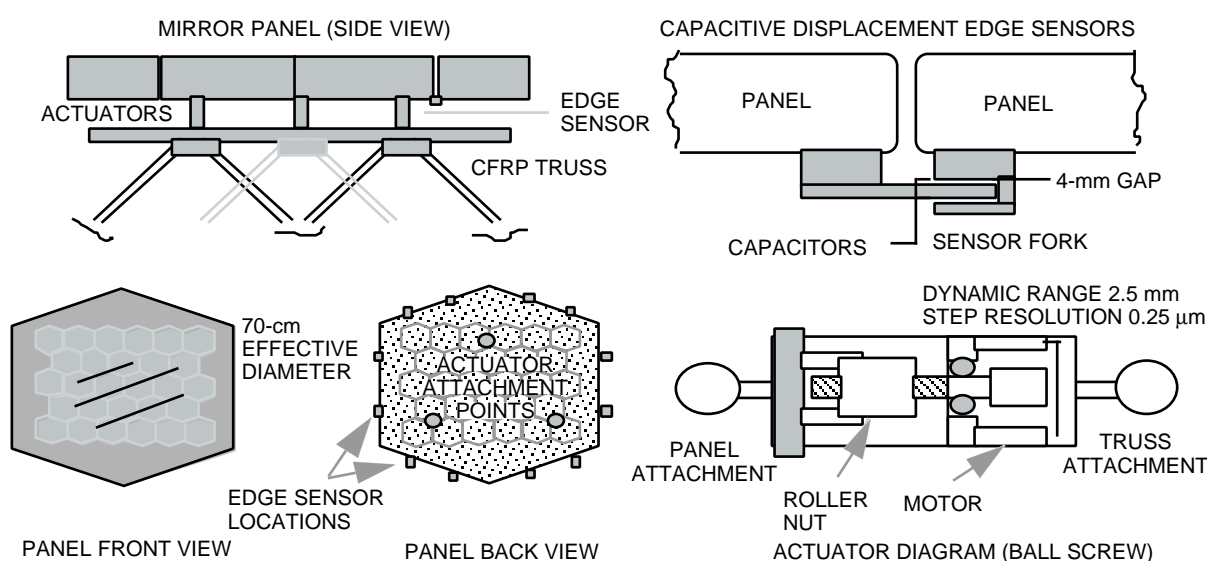


Fig. B-1. Panel-mounting configuration for the primary mirror.

⁷ *Ground Based Advanced Technology Study (GBATS)*, op cit.

Table B-1. Input parameters to the OPTI program.

Parameter	Value
Transmitter	
Transmitter average power, W	1.35
Laser light wavelength, μm	1.054
Transmitter antenna diameter, m	0.25
Transmitter obscuration diameter, m	0.03
Transmitter optics efficiency	0.7
Transmitter pointing bias error, μrad	1
Transmitter root mean square (rms) pointing jitter, μrad	1
Modulation extinction ratio	0.1×10^6
Receiver	
Receiver aperture diameter, m	10.0
Receiver obscuration diameter, m	1
Receiver optics efficiency	0.7
Detector quantum efficiency	0.38
Narrowband filter transmission factor	0.6
Filter spectral bandwidth, μm	10^{-4}
Detector diameter field of view, μrad	100
APD gain	280
Noise temperature, K	350
Load resistance, ohms	2000.0
APD effective ionization ratio	0.7×10^{-2}
APD surface leakage current, A	0.1×10^{-8}
APD bulk leakage current, A	0.1×10^{-11}
Operational	
Alphabet size	512
Data rate, kbps	267
Link distance, AU	2.7
Required link bet-error rate	0.4×10^{-1}
Atmospheric transmission factor	0.7
Dead time, μs	16.3
Slot width, ns	34
Noise sources	
Mars receiver-to-source distance, AU	2.7
Additional noise sources	
Day-sky high radiance, $\text{W}/\text{M}^2/\text{SR}/\text{A}$	0.011

An alternative receiving system, using a 3.5-m aperture derived from current commercial practice [8], also was considered. This terminal, while much smaller in collecting area than the 10-m aperture, also has a better surface and thus collects significantly less background light than the larger 10-m photon bucket. For daylight operation, the net effect is a receiving sensitivity that is about one-third of that of the much larger aperture.

Table B-2. Output of the OPTI program.

Parameter	Back-up value	Value	Value, dB
Laser output, W	—	1.35	31.3 dBm
Minimum required peak power, W	0.13×10^4	—	—
Transmitter antenna gain	—	0.43×10^{12}	116.3
Antenna diameter, m	0.250	—	—
Obscuration diameter, m	0.030	—	—
Beamwidth, μrad	7.041	—	—
Transmitter optics efficiency	—	0.700	−1.5
Transmitter pointing efficiency	—	0.732	−1.3
Bias error, μrad	1.000	—	—
RMS jitter, μrad	1.000	—	—
Space loss, 2.7 AU	—	0.431×10^{-37}	−373.7
Receiver antenna gain	—	0.880×10^{15}	149.4
Antenna diameter, m	10.000	—	—
Obscuration diameter, m	1.000	—	—
Field of view, μrad	100.00	—	—
Receiver optics efficiency	—	0.760	−1.2
Narrowband filter transmission	—	0.600	−2.2
Bandwidth, \AA	1.000	—	—
Detector quantum efficiency	—	0.380	−4.2
Atmospheric transmission factor	—	0.770	−1.5
Received signal power, W	—	0.398×10^{-11}	−84.8 dBm
Received background power, W	0.237×10^{-8}	—	—
Photons/joule	—	0.531×10^{19}	157.2 dB/mJ
Detected signal photo-electron (PE)/s	—	0.801×10^7	68.3 dB-Hz
Symbol time, s	—	0.337×10^{-4}	−44.7 dB-Hz
Detected signal PE/symbol	—	269	23.5
Required signal PE/symbol	—	135	21.0
Detected background PE/slot	162	—	—
Margin	—	2.00	2.5

II. Uplink Transmitter System

A schematic of the ground transmitter station is shown in Fig. B-2. It consists of a high-power laser propagated through a subaperture of a standard astronomical-quality 1.5-m telescope. Although the telescope's principal use is to transmit uplink commands to the satellite, it also is used to acquire and track the spacecraft and to collect downlink telemetry during the transfer-orbit phase. Coarse pointing is accomplished using the telescope control mechanism. A two-axis mirror controlled through the telescope control computer is used for fine-pointing adjustment of the laser beam. Approaches for pointing the telescope to the spacecraft depend on the phase of the trajectory. During the near-Earth phase, telescope

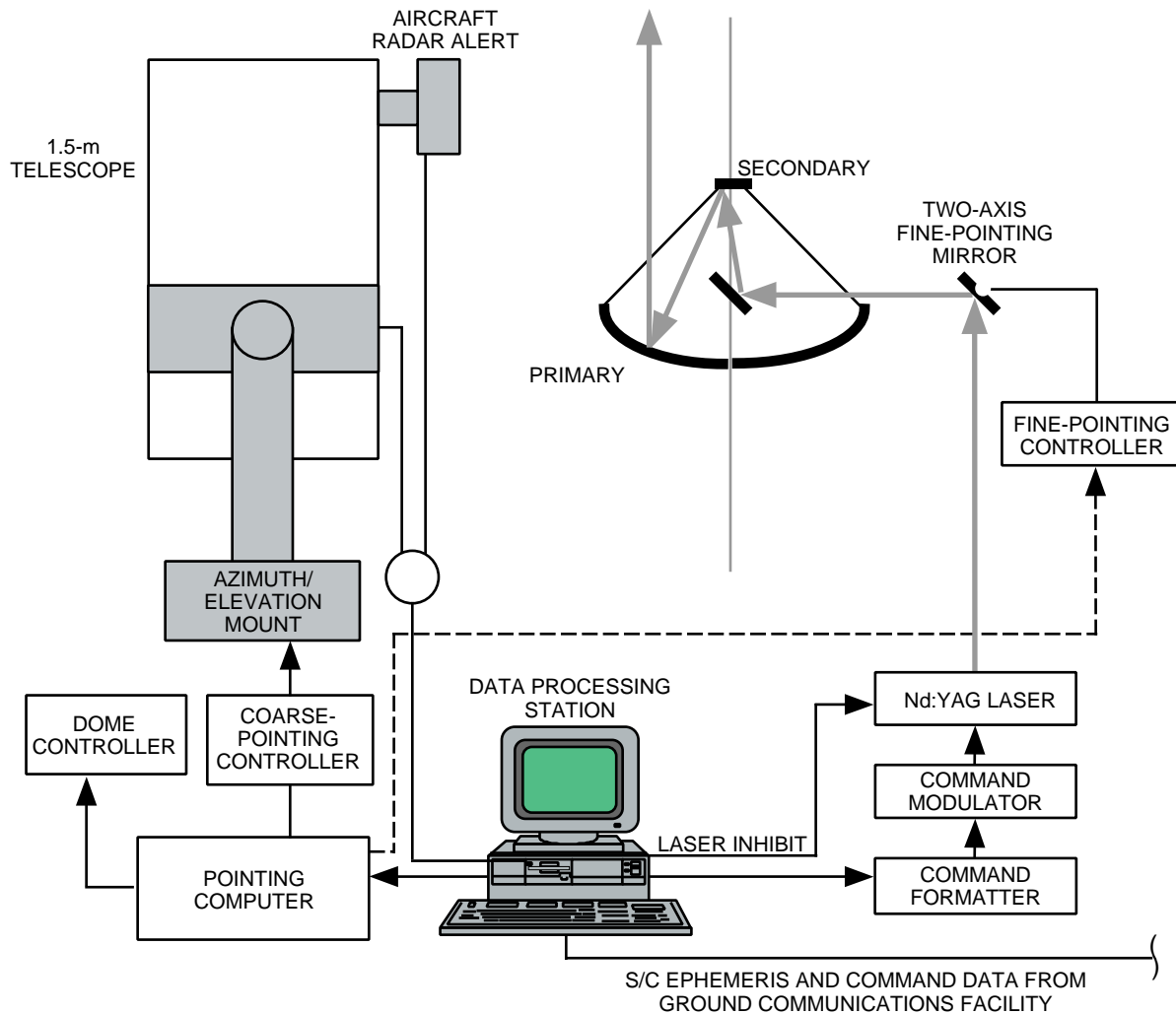


Fig. B-2. Schematic of the transmitter showing the telescope control and data flow for uplink command.

pointing is accomplished using a spacecraft ephemeris file that has been generated from tracking data. In the deep-space phase, guide stars are used as pointing references [2]. This latter requirement defines the figure and, hence, cost of the transmitter telescope.

Because of the possible hazard posed by the uplink laser to aircraft passengers and crew, the ground transmitter station is equipped with an aircraft detection radar unit. This unit is coaligned with the beam propagation axis and is interlocked with the laser emission system. The radar system interrupts laser transmission when an aircraft is detected. The uplink laser is based on a commercially developed diode-pumped laser technology and is a 10-J-per-pulse, 100-Hz repetition rate, Q-switched Nd:YAG laser operating at the 1064-nm fundamental (or 532-nm harmonic) laser wavelength. The infrared uplink wavelength reduces the effects of atmospheric attenuation and scintillation and, at the same time, is sufficiently removed from the 1053-nm downlink that it provides adequate wavelength isolation between the transmit and receive beams in the spacecraft's optical train.

The link analysis for the uplink transmission also has been performed by the OPTI software. Example uplink link-analysis parameters appear in Table B-3. The laser beam illuminates a 20-cm subaperture of the telescope primary to mitigate the effect of uplink scintillation and beam wander. Subaperture beam propagation has been used successfully in the two JPL-led laser communications

Table B-3. Uplink design parameters summary.

Parameter	Value
Transmitter	
Transmitter average power, W	1000
Wavelength, μm	1.06
Transmitter diameter, cm	20
Transmitter obscuration, cm	N/A
Transmitter optics efficiency	0.9
Pointing-bias error, μrad	5
Pointing jitter, μrad	5
Beamwidth, μrad	35
Operational	
Alphabet size	256
Data rate, kbps	0.6
Link distance, AU	2.7
Atmospheric transmission	0.87
BER	10^{-5}
Link margin, dB	11
15-cm spacecraft receiver (1 Gb/day)	

demonstrations: the Galileo Optical Experiment (GOPEX) [3] with the Galileo spacecraft and the Ground/Orbiter Lasercomm Demonstration (GOLD) [4] with the Japanese Engineering Test Satellite VI (ETS-VI). Transmitter stations are located above a 2-km altitude to reduce further the effects of scintillation and beam wander on the uplink. The sites are assumed to have 4 arcsec of daytime seeing or a Fried atmospheric coherence length of 3 cm at $0.5 \mu\text{m}$. Under these conditions, the expected beam wander has a $1\text{-}\sigma$ value ranging from $9 \mu\text{rad}$ to $21 \mu\text{rad}$, as the zenith angle is increased from zero to 60 deg. The link was designed with a beam divergence of approximately $35 \mu\text{rad}$ (i.e., $1.5\text{-}\sigma$ for the beam wander at a 60-deg zenith angle) to accommodate signal fades up to 11 dB for the 15-cm spacecraft receiver telescope and fades up to 13 dB for the 25-cm receiver telescope.

Although not considered in the current analysis, recent GOLD experiments [5] have demonstrated that there is a distinct reduction in uplink scintillation when the uplink beam is propagated through multiple subapertures that are separated by greater than r_o with relative path delays greater than the laser's coherence length. Both two-beam and four-beam approaches were used during the GOLD experiment to demonstrate uplink beacon scintillation reduction.

III. Data Processing, Electronics, and Facilities

Each optical station is designed to be fully automated and will contain three Sparc 20 and two Hewlett Packard (HP) workstations, a weather analysis terminal, pointing computers and controllers, and a timing system. The facilities will consist of a 2300-square-foot prefabricated modular building housing the optics, computer archiving, and the control room, as well as an area for maintenance tasks. The aperture and dome will be mounted on concrete pads adjacent to the facility.

IV. Ground Network Development and Operations Costing Process

Estimation of the costs for development and operations of the optical communications ground facilities used the methodology employed in the GBATS study; the study contains a detailed description of the

methodology, which will not be repeated here.⁸ The method relies upon an engineering breakdown of the work needed, guided by analogies in the RF domain of the DSN. The breakdown extended to a point where order-of-magnitude values could be fixed using vendor quotes, analogies, and engineering judgment or extrapolation from the GBATS results. The cost estimate was developed first for a stand-alone optical communications station, which was then used as a building block for the several subnet configurations of interest. The next step consisted of producing cost estimates for the development and deployment of multiple-station subnets, including required common support facilities such as the centralized Network Operations Control Center (NOCC). This study included three concepts: seven linearly dispersed stations, a set of three stations in the continental U.S., and a double/single station design. The assumed development schedule duration was 5, 4, and 3 years, respectively. Program-level costs include program management, system engineering, hardware and software design engineering, transport, and documentation, in addition to the basic construction elements and applicable burdens. It was assumed that the development would be done in a multiple subcontract mode, with JPL providing the overall management and integration.

Appendix C

Optical Communication Link Control Table Uncertainties

The expected daily data volume is directly dependent on the data rate that is afforded by the laser communications terminal. The data rate in turn is dependent on the required link margin. The link margin was calculated in the following manner [9]:

- (1) The atmospheric attenuation for the link was determined from the atmospheric visibility monitoring (AVM) measurements taken by JPL at the Table Mountain Facility (TMF). These curves give the cumulative probability distribution of the atmospheric attenuation at zenith at the 860-nm wavelength. AVM data indicate a 59-percent probability that the atmospheric attenuation is less than 2 dB (at 860 nm).

The downlink wavelength in this study is 1050 nm. We used the LOWTRAN propagation model to determine the relative scaling of the transmission of the atmosphere from 860 to 1050 nm. The model predicted an increase in atmospheric transmission of 4 percent (i.e., a 1.8-dB atmospheric transmission loss) at 1050 nm. The atmospheric loss at other than zenith angles was calculated using the expression $l = -10 \log\{T_o^{secq}\}$. These results were used in the link analysis to determine the optimum elevation for initiating the downlink.

- (2) Link analysis calculations were performed initially (for example, for the 10-Gb daily data volume) using the OPTI program to determine the optical communication link parameters (transmit laser power, instrument throughput efficiency, atmospheric attenuation, etc.) for a link margin of 0 dB.

⁸ *Ground Based Advanced Technology Study (GBATS)*, op cit.

- (3) Favorable and adverse tolerances were then assigned to each of the input parameters (to the link analysis program). Subsequently, the mean and variance for each component parameter were calculated. The $1\text{-}\sigma$ link variance corresponds to the square root of the sum of the component variances. The required data link margin (based on allocated adverse and favorable tolerances) was then set at $2.2\text{ }\sigma$ (corresponding to a confidence level of 98.6 percent). Following the above procedure, which is shown in Table C-1, we find that $2.2\text{ }\sigma$ is equal to 2.5 dB. In the OPTI program, the required link margin was then changed to (the $2.2\text{ }\sigma$ value of) 2.5 dB, and the data rate was reduced to produce that margin.
- (4) Using plots (elevation angle versus time) of coverage of Mars by a (worldwide) linearly dispersed optical subnet (LDOS) of stations, an optimum optical telemetry load line was established. To determine the optimum load line, the following procedure was used: (1) calculate the data rate for different elevation angles (from 20 to 70 deg, with a corresponding atmospheric transmission loss for each angle) and (2) calculate the expected data volume (EDV) from the relationship

$$EDV = R \sum P_i \times T_i$$

where R is the data rate, P_i is the probability of availability for a given station (see the GBATS study), and T_i is the corresponding coverage time (for the specific elevation angle). The optimum telemetry load line corresponds to an elevation angle that provides the required data volume (0.1, 1.0, or 10.0 Gb/day) with the least number of ground receiving stations.

Table C-1. Sample design control table.

Component parameter	Design value	Favorable tolerance	Adverse tolerance	Variance	Distribution
Laser power, dBm	28.3	1	-1.4	0.48	Uniform
Transmitter optics efficiency, dB	-1.55	0.3	-0.7	0.08	Uniform
Transmitter pointing efficiency, dB	-1.3	0.4	-1	0.05	Gaussian
Transmitter antenna gain, dB	111.3	0	-4	0.44	Gaussian
Receiver optics efficiency, dB	-1.2	0.4	-0.5	0.07	Uniform
Detector quantum efficiency, dB	-4.2	0	-0.5	0.01	Gaussian
Filter transmission factor, dB	-2.2	0.4	-0.4	0.02	Gaussian
Atmospheric transmission factor, dB	-3.3	0.6	-0.6	0.04	Gaussian
Receiver antenna gain, dB	155.4	0.8	-1	0.09	Gaussian
Space loss, dB	-373.7	0	0	0.00	—
Received signal power, dBm	-87.45	—	—	—	—
Required signal power, dBm	-87.45	—	—	—	—
Margin, dB	0	—	—	—	—
Sum of variances	—	—	—	1.28	—
Square root of variance ($1\text{ }\sigma$)	—	—	—	1.13	—
$2.2\text{ }\sigma$ (>98.6-percent confidence), dB	—	—	—	2.50	—
Data rate, kbps	267	—	—	230.33	—

Appendix D

Optical Communication Transceiver Mass and Power

The details of the mass and power estimation for the 25-cm, 1.35-W optical communication transceiver terminal are presented in Table D-1. Probable error and redundancy factors are included as applicable. Acronyms/abbreviations used in the table include the Mars Observer laser altimeter (MOLA), communication(s) (COM), beamsplitter (B/S), silicon carbide/aluminum (SXA), General Scanning (GS), left-hand design (LHD), and redundancy (redun.).

Table D-1. Optical communication transceiver mass and power.^a

Component	Qty	Redun. factor	Mass, g			Power, W		Notes, assumptions, references
			Mean	Error (±)	Redun. mean	Mean	Error (±)	
Laser subsystem								
Semiconductor diode laser	2	2	80	20	169	9	2	Weighed, SDL Inc., MOLA
Diode laser electronics	1	2	400	100	800	0	0	Weighed comparable optics
Beam-shaping optics	5	2	30	10	60	0	0	Weighed comparable optics
Laser crystal	5	2	10	0	20	0	0	Weighed
Q-switch	1	2	20	0	40	0	0	Weighed
Q-switch/modulator electronics	1	2	100	25	200	1.2	0.2	Weighed
Laser cavity optics	4	2	20	5	40	0	0	Weighed
Mounts and hardware	1	2	400	100	800	0	0	Estimated comparable optics
Thermal management assembly	1	2	500	50	1000	3.5	1	Estimated based on diode pump
Laser system subtotal	—	—	1560	154	3120	13.70	2	Comparable to Clementine's laser
Transmitter/receiver aperture								
Telescope	1	1	1800	300	1800	0	0	All SXA foam material
Telescope baffles	1 set	1	400	100	400	0	0	Estimated
Beam-shaping optics	4	1	110	20	110	0.5	0.2	Weighed comparable optics
Telescope aperture filter	1	1	10	0	10	0	0	Weighed
Mounts and hardware	2	1	500	100	500	0	0	Interface plate, estimated
Transmitter/receiver aperture subtotal	—	—	2820	332	2820	0.5	0.2	—
Acquire/track/point/COM								
Acquisition/tracking detector	1	2	50	10	100	1.5	0.4	APS array
COM detector assembly	1	2	20	5	40	1.1	0.3	Clementine and MOLA
Fine-pointing mirror assembly	1	1	200	50	200	1	0.3	GS TABS model III and LHD model F020
Optics (lenses, B/S etc.)	6	1	120	10	120	0	0	Weighed comparable optics
Mounts and hardware	1	1	200	100	200	0	0	Estimated
Acquire/track/point/COM subtotal	—	—	590	113	660	3.6	0.58	—
Thermal/mechanical								
Shielding and control	1 set	1	400	—	400	0.5	0.1	Estimated
Cables/harness/connector	1 set	1	500	—	500	0	0	Estimated
Thermal/mechanical subtotal	—	—	900	0	900	0.5	0.1	—
System subtotal	—	—	5870	383	7500	18.30	2.33	—
Other								
Vibration isolation flexure	1	1	600	100	600	0.00	0.00	Three-axis
Lasercomm control unit	1	1	400	100	400	8	1	Assumed a MOPS6000
Power conditioning unit	—	—	—	—	—	3.95	0	Efficiency = 0.85, mass considered above
Miscellaneous	1	1	500	—	500	0	—	—
Other subtotal	—	—	1500	141	1500	11.95	1	—
Totals	—	—	7370	408	9000	30.25	2.54	1-σ error
Weight 9.0 kg, power 30.3 W								
a Date prepared, April 1995; maximum link distance, 2.7 AU; average laser power, 1.35 W; laser peak power, 1.3 kW; slot width, 34 ns; link, Mars; data rate, 200 kb/s; data volume, 10 Gb/day; transmitter aperture, 0.25 m; receiver aperture, 10 m; technology cutoff date, December 1996; day/night time, day; zenith angle, 70 deg; BER (coded), 10 ⁻⁵ ; margin, 3 dB.								